Journal of Colloid and Interface Science 354 (2011) 461–466

Contents lists available at ScienceDirect

Journal of Colloid and Interface Science

www.elsevier.com/locate/jcis

Preparation of semiconductor-enriched single-walled carbon nanotube dispersion using a neutral pH water soluble chitosan derivative

Choolakadavil Khalid Najeeb, Jingbo Chang, Jae-Hyeok Lee, Minsu Lee, Jae-Ho Kim *

Department of Molecular Science and Technology, Ajou University, Gyeonggi-do, Suwon 443-749, Republic of Korea

ARTICLE INFO

Article history:
Received 17 July 2010
Accepted 28 October 2010
Available online 2 November 2010

Keywords:
Single-walled carbon nanotubes
Debundling
Semiconducting nanotubes
Individual dispersion
Chitosan derivative
Biocompatible

ABSTRACT

Debundling and selective dispersion of semiconducting single-walled carbon nanotubes (SWNTs) has been demonstrated using a neutral pH water soluble chitosan derivative, N-acetylated chitosan (NACHI), which is synthesized by controlled N-acetylation of chitosan using acetic anhydride. The SWNT–NACHI supernatant solution demonstrated semiconductor-enriched property owing to the preferential adsorption of N-groups of the NACHI on semiconducting nanotubes with a fairly weak charge transfer. The dispersion of nearly individualized SWNTs achieved by surface modification of nanotubes with a biocompatible polymer can be utilized for electronic and biomedical applications such as field effect transistor, biosensor, cell culture medium and SWNT-biomacromolecule hybrid materials.

1. Introduction

Single-walled carbon nanotubes (SWNTs) have drawn great attention of researchers on account of their unique electrical, mechanical, and thermal properties which are significant to various potential technological applications [1–5]. As produced SWNTs exist as large bundles or ropes of 30–50 nm diameters due to the strong intertube van der Waals attraction, along with the hydrophobic property make them insoluble in most of the common solvents and in polymer matrix [6]. As synthesized SWNTs usually contain about 1/3 metallic and 2/3 semiconducting SWNT species. Separation as well as individual solubilization of SWNTs is essential for many of the realistic applications which are particular to one or the other type of nanotubes in order to explore their unique and extraordinary properties. There have been tremendous amount of efforts for the separation, solubilization and hence the processing of SWNTs by means of covalent, noncovalent, ionic or free radical modifications of nanotube surfaces [7–11]. The noncovalent approach is considered to be the most promising technique, because it allows surface modification of carbon nanotubes (CNTs) without much disturbing the π-system of the graphene sheet, therefore it preserves intrinsic electronic structure of the nanotubes [12]. Different types of surfactants, aqueous and organic solutions of polymers have been widely employed for the solubilization and hence processing of CNTs [13–17]. In order to separate semiconducting from metallic tubes, several methods including density gradient induced centrifugation, AC dielectrophoresis, gel electrophoresis, selective adsorption of semiconducting SWNTs on agarose gel, selective electrical breakdown of metallic CNTs, selective flocculation assisted by octadecylamine or porphyrins have been investigated [18–24]. Recently, Cao et al. demonstrated percolation theory based methods to reduce the metallic conduction paths in a random network CNT circuit [25]. The nanotubes dispersed in biocompatible media are of special interest for applications such as biosensor, template for cell culture, SWNT-biomacromolecule hybrid, etc. Various biomolecules, biosurfactants and biopolymers including DNA, proteins, poly(L-lysine), starch, gelatin, steroids and chitosan have shown capability for the effective debundling and individual dispersion of SWNTs in water [26–30].

In this contribution, we present debundling and diameter selective dispersion of small diameter SWNTs possessing semiconductor-enriched property with the assistance of a neutral pH water soluble chitosan derivative. The chitosan, (poly-β-(1–4)-D-glucosamine), is a deacetylated product of chitin and is a naturally abundant polysaccharide. However chitosan has been used for various functional materials, including biomaterials, its applications are limited because of insolubility in water, it can only be dissolved in acidic medium [31,32]. The chitosan has demonstrated capability for dispersing SWNTs in acidic medium and it also has shown tendency to preferentially disperse smaller diameter nanotubes [33,34]. Recently, Zhang et al. reported the debundling and individual dispersion of SWNTs in neutral pH aqueous solutions of chitosan derivatives such as O-carboxymethyl chitosan and O-carboxymethyl chitosan modified with poly(ethylene glycol) [35]. Herein, we demonstrate effective debundling and suspension of

* Corresponding author. Fax: +82 31 219 2516.
E-mail address: jhkim@ajou.ac.kr (J.-H. Kim).

0021-9797/$ - see front matter © 2010 Elsevier Inc. All rights reserved.
doi:10.1016/j.jcis.2010.10.064

individual or thin bundles of semiconductor-enriched SWNTs using a neutral pH water soluble chitosan derivative, N-acetylated chitosan (NACHI), which is synthesized by a simple functionalization process reported in literature [31]. The lone pair of electrons on the electron rich N-groups such as amine and amide groups of NACHI plays a vital role in the isolation of SWNTs into thinner bundle or individual tubes as well as selective dispersion of semiconducting nanotubes [24,36]. Compared to unsorted nanotubes, the semiconductor-enriched SWNTs hold great potential for applications such as thin film transistors and display applications owing to their high mobility, high ratio of semiconductor nanotubes, and compatibility for room-temperature processing [37]. The suspension of nearly individualized semiconductor-enriched nanotubes obtained by wrapping with biocompatible polymer opens up new prospects for diverse electrical and biomedical applications including thin film transistors, biosensor, SWNT-biomacromolecule hybrids, cell culture, and drug delivery applications.

2. Materials and methods

2.1. Materials and instrumentation

The SWNTs synthesized by HiPco process were purchased from Unidym, USA. Low molecular weight chitosan (degree of deacetylation: 75–85%, $M_n = 1.2 \times 10^5$ Da), acetic anhydride, pyridine and sodiumdodecylbenzenesulfonate (SDBS) were purchased from Sigma–Aldrich. Acetic acid, acetone and ethanol were obtained from Samchun chemicals, Seoul, Korea.

A cup-horn type ultrasound sonicator (Sonics, VCX 750, Vibracell™, USA) was used for the preparation of SWNT dispersions. The Fourier transform-infrared (FT-IR) spectra of polymer and SWNT–NACHI samples were recorded on a Nicolet OMNIC 6700 FT-IR spectrometer (Thermo scientific, USA). Scanning electron microscope (SEM) images of SWNT dispersions drop-casted on silicon (Si) substrate were obtained using a LEO SUPRA 55, Genesis 2000 (Carlzeiss instrument, Germany) operated at 1.5 kV. Transmission electron microscope (TEM) image of SWNT supernatant dropped and dried on 400 mesh copper grid (G400, Gilder 400 mesh Grid, Cu, Ted Pella, Inc. CA) was obtained using a JEOL high resolution transmission electron microscope. Atomic force microscope (AFM) images were obtained using a silicon AFM tip with XE-100 instrument (Park system, Korea) in non-contact mode at atmospheric condition. Ultraviolet–visible–near infrared (UV–vis–NIR) absorption measurement was performed using a JASCO-V530 UV–vis–NIR spectrometer (Japan). Raman spectra were recorded on a Dongwoo 320i instrument using 785 nm diode laser beams with 1 s exposure time. The Raman fluorescence spectra were obtained using Raman RXN Kaiser Optical Systems. Inc. (USA) at an exposure time of 10 s at an excitation wavelength of 785 nm. The current–voltage characteristics of thin films were recorded using a Keithley 2612 SYSTEM sourcemeter.

2.2. Synthesis of N-acetylated chitosan

The water soluble chitosan derivative, NACHI, was prepared by controlled N-acetylation of chitosan according to a method previously reported in literature [31]. Briefly, low molecular weight chitosan sample (1 g) was dissolved in 25 mL of 2.8% acetic acid in a flask equipped with a plug, 25 mL of ethanol was added into it and stirred well. Pyridine (approx. 8 mL) was dropped into the mixing solution until the solution became clear. Acetic anhydride (10 mL) was charged into the reaction mixture with continuous stirring. After it was stirred for 4 h at ambient temperature, the reaction mixture was precipitated with ethanol. The precipitate was then washed with excess acetone to remove excess reagents.

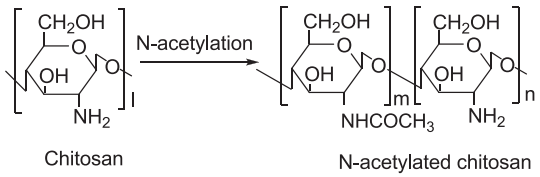

Scheme 1. Preparation of water soluble N-acetylated chitosan.

The derivatized chitosan sample was dried overnight at 50 °C in a hot air circulating oven. The degree of deacetylation of the product was estimated to be 49.7 by acid–base titration [31]. Characterization of the derivatized sample was conducted by FT-IR spectroscopy. A schematic representation for the synthesis of water soluble chitosan derivative is shown below (Scheme 1).

2.3. Preparation of SWNT dispersion

In a typical experiment, 30 mg SWNTs were immersed into 100 mL aqueous solution of NACHI (5 mg/mL) and ultrasonicated using a cup-horn type ultrasound sonicator at 200 W for 10 min and 540 W for 30 min. The temperature of sonication bath was maintained below 10 °C by putting ice to avoid structural damages which may occur due to excessive heating effects. The dispersion was then centrifuged at 15,000 rcf (relative centrifugal force) for 5 h to remove aggregates and bigger bundles. The greenish colored supernatant solution was carefully collected. A reference sample was prepared using aqueous solution of an anionic surfactant, SDBS, under the same experimental conditions. Characterizations of the SWNT dispersions were carried out by SEM, TEM, AFM, UV–Vis–NIR absorption spectroscopy, Raman spectroscopy and by electrical measurements.

3. Results and discussion

3.1. Characterization of N-acetylated chitosan

To confirm the functionalization, FT-IR spectra of pristine chitosan and NACHI samples were recorded using KBr pellet in transmittance mode. Fig. 1 shows that the characteristic absorption bands of chitosan corresponding to –CO–NH_2 vibrations at 1655 and 1592 cm^{-1} became more enhanced when the chitosan was functionalized with acetic anhydride. Furthermore, the band II of amide group at 1592 cm^{-1} marked noticeable enhancement and a peak shift towards lower wave number region (1558 cm^{-1}), which indicate that the functionalization has been occurred at the amino groups of chitosan. N-acetylation causes destruction of intermacromolecular hydrogen bonds and interchain hydrogen bonds, which alter the secondary structure of chitosan, decreasing its crystallinity and unfolding its molecular chains, which in turn improve the solubility of NACHI in water [31].

3.2. Characterization of SWNT–NACHI dispersion

The characterization and evaluation of SWNT–NACHI dispersions were carried out in comparison with a reference sample prepared using an anionic surfactant SDBS under the same experimental conditions. Optical photograph of SWNT dispersions, which are used in this study, are shown in Fig. 2. The SWNT–NACHI supernatant has a greenish color, while the uncentrifuged SWNT–NACHI dispersion and SWNT–SDBS supernatant are black colored. The greenish coloration is due to the supernatant mainly consists of smaller diameter nanotubes, which is reflecting the separation of SWNTs [20].

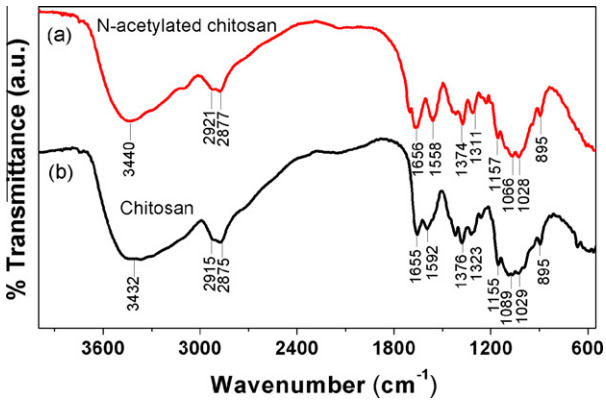

Fig. 1. FT-IR spectra of (a) N-acetylated chitosan and (b) pristine chitosan sample using KBr pellet.

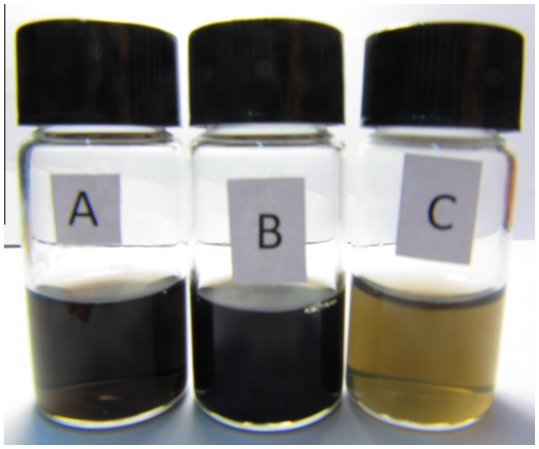

Fig. 2. Optical photograph of (a) SWNT–SDBS supernatant, (b) uncentrifuged SWNT–NACHI suspension, and (c) green colored SWNT–NACHI supernatant. (For interpretation of the references to colour in this figure legend, the reader is referred to the web version of this article.)

The SEM image of SWNT–NACHI dispersion drop deposited on Si wafer is shown in Fig. 3a. The SWNT film was washed with water prior to the SEM measurements to remove excess polymer from the surface. The SEM image shows that the nanotubes are exfoliated into smaller bundles and are homogeneously dispersed. The straight rod-like appearance of nanotubes implies that the tube surface may be wrapped with rigid polymer chains and, therefore it is believed that the originally flexible nanotubes turned into rigid structure. Fig. 3b shows the TEM image of SWNT–NACHI supernatant deposited on a TEM grid. To prepare sample for TEM analysis, a small drop of sample was dropped onto a 400 mesh amorphous carbon supported copper grid and dried at room temperature. The grid was rinsed several times with DI water to remove polymer from the SWNT surface. The TEM image illustrates that the SWNT bundles were exfoliated to smaller bundles as well as individual nanotubes with diameters ranging from 1.5 to 2 nm.

The AFM image of SWNT–NACHI supernatant further demonstrated that the nanotubes are present as individual nanotubes as well as thin bundles. The height of nanotubes measured by AFM represents the bundle diameter of SWNTs. Fig. 4a shows that the height profile for SWNT–SDBS supernatant represented relatively bigger bundle diameters, in the range of 2.5–4 nm, because the typical size of SDBS micelle is 3.5 ± 0.5 nm [38]. The diameter of most of nanotubes in the SWNT–NACHI supernatant from the height profile was found to be 1.2–1.4 nm, demonstrating that most of the nanotubes are isolated by selective adsorption of NACHI on smaller diameter nanotubes (Fig. 4b). Presence of thin bundles consisting of 2–3 nanotubes can also be seen in the AFM image of SWNT–NACHI sample.

Fig. 5a shows the UV–Vis–NIR absorption spectra of SWNT–NACHI dispersion before and after centrifugation in comparison with that of SWNT–SDBS supernatant. The SWNT–NACHI supernatant demonstrated well-resolved narrow peaks (solid-line), which are attributed to inter-band transition between van Hove singularities in the density of states of individual SWNTs, indicating the presence of individually dispersed SWNTs or thin bundles. Conversely, the broad absorption bands of uncentrifuged SWNT–NACHI and SWNT–SDBS supernatant samples designate the presence of relatively larger bundles (dotted lines). The absorption bands in the wavelength range from 400 to 600 nm represent the lowest energy M_{11} van Hove transition of metallic SWNTs, from 550 to 800 nm represent the second van Hove transition of semiconducting SWNTs (S_{22}) and from 800 to 1400 nm correspond to the first van Hove transition of semiconducting SWNTs (S_{11}). The S_{11} peaks marked increase of intensity as they are easily affected by the SWNT chemical environment [35].

Fig. 5b–d represents Raman spectra of SWNT–NACHI supernatant solution, SWNT–NACHI dispersion before centrifugation, and SWNT–SDBS supernatant. The diameter-dependant radial breathing mode (RBM) band of SWNT Raman spectra at 785 nm excitation provides information about the degree of aggregation of SWNTs according to the fact that the RBM band at ca. 267 cm^{-1} of (10, 2) SWNTs is very low or absent in the isolated SWNTs. If there is aggregation of nanotubes present in the dispersion, it is

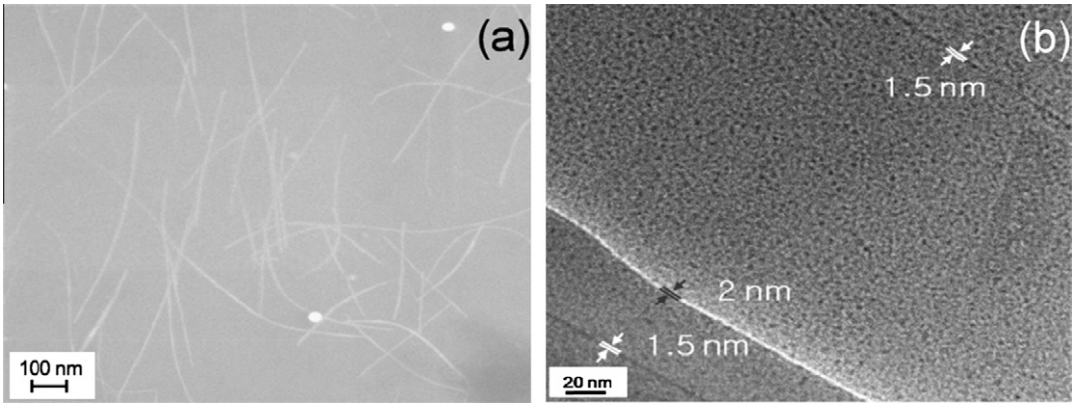

Fig. 3. SEM and TEM image of SWNT–NACHI supernatant: (a) SEM image of SWNT–NACHI thin film drop deposited on Si substrate and (b) TEM image of SWNT–NACHI dropped on 400 mesh TEM grid.

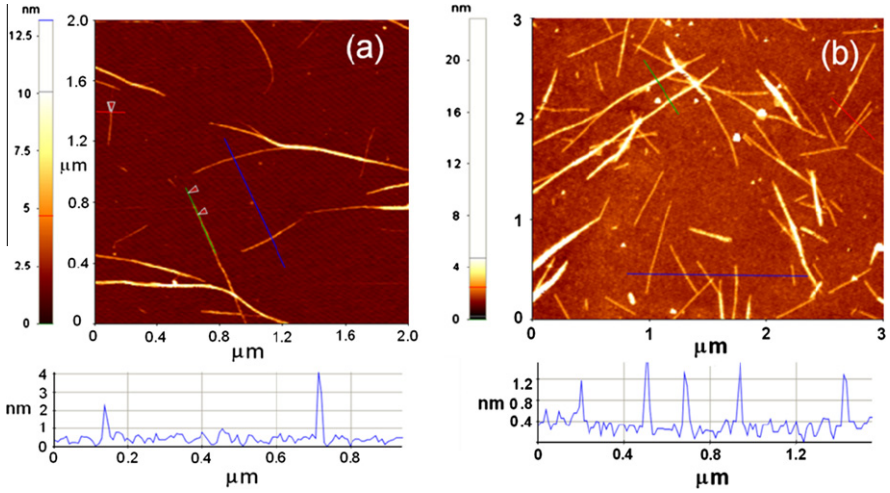

Fig. 4. AFM images and height profiles of: (a) SWNT–SDBS supernatant and (b) SWNT–NACHI supernatant thin film drop deposited on Si substrate.

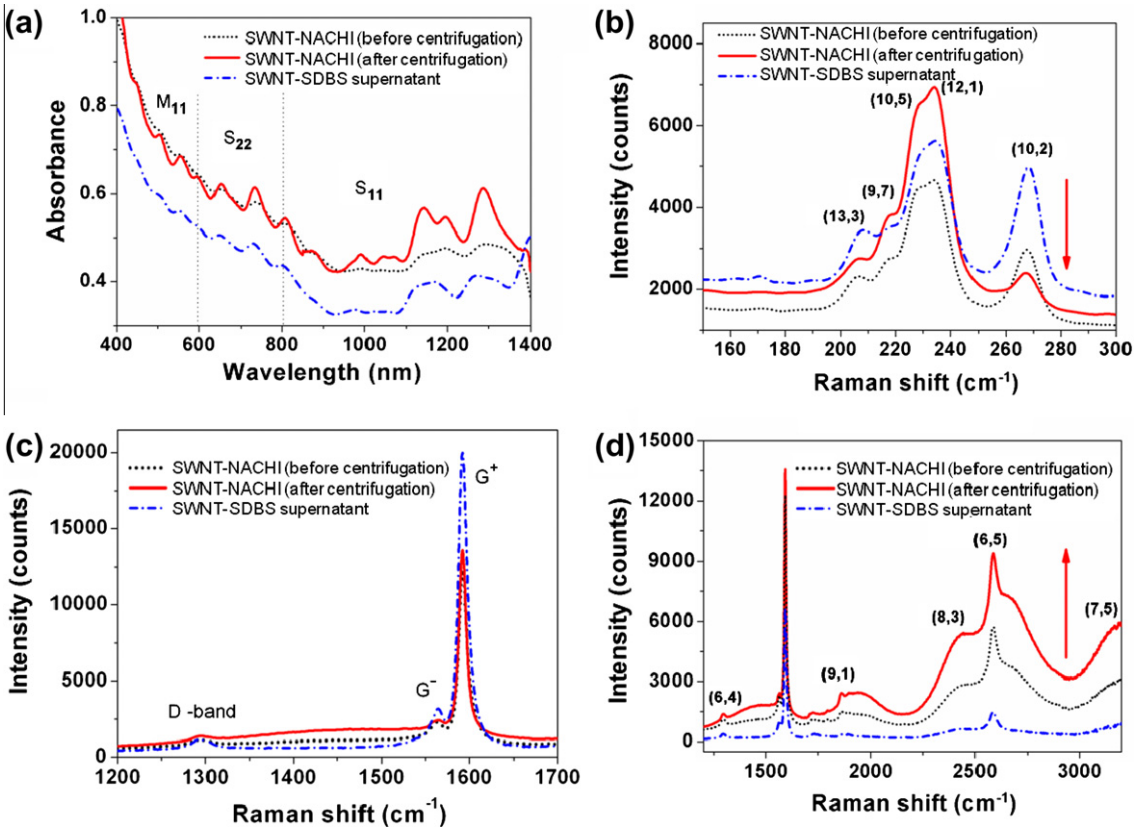

Fig. 5. (a) UV–Vis–NIR absorption spectra of SWNT–NACHI before and after centrifugation and SWNT–SDBS supernatant and (b)–(d) Raman spectra of the same samples.

attributed that the off-resonated (10, 2) SWNT RBM peaks, commonly known as "roping peaks", begin to resonate [39]. In Fig. 5b, the roping peak at ca. 267 cm^{-1} analogous to the aggregation status of SWNTs was considerably low for the SWNT–NACHI supernatant (solid-line) compared to that of uncentrifuged sample as well as the SWNT–SDBS supernatant (dotted lines) indicating the presence of isolated nanotubes and thin bundles in the supernatant. The RBM peaks observed at ca. 207, 216, 227, 236, and 267 cm^{-1} are ascribed to the semiconducting (13, 3), (9, 7), (10, 5), (12, 1) and (10, 2) SWNTs, respectively.

Fig. 5c shows that the G^+ band of SWNT–NACHI supernatant was slightly narrow and the G^- band of was considerably diminished (solid-line) compared to other two samples indicating that more semiconducting SWNTs exist in supernatant. It is known that nitrogen containing functional groups such as amines and amides possess significant affinity for SWNT physisorption with fairly weak charge transfer on the SWNT side wall due to the high nucleophilicity of the N-based groups [24,40]. Moreover, materials with amine group have demonstrated slight preference to attach on semiconducting nanotubes [36]. The NACHI possess nucleophilic

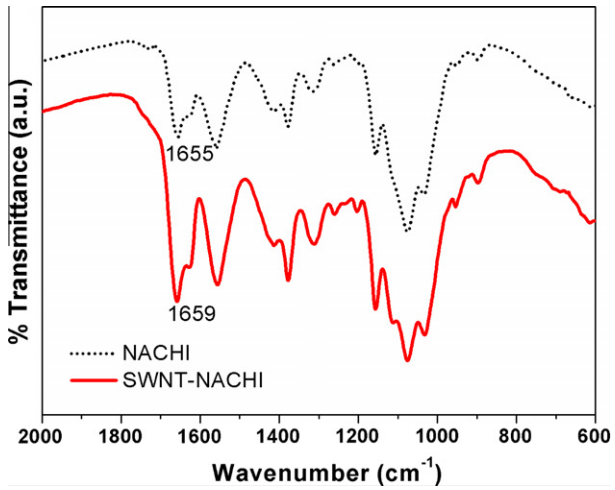

Fig. 6. FT-IR spectra of NACHI (dotted line) and SWNT–NACHI (solid-line) solution drop deposited on Si substrate.

groups such as amide and amine, therefore it is assumed that the NACHI selectively adsorbed on semiconducting nanotubes with slight preference and hence the supernatant is enriched with semiconducting nanotubes. The free electron pair in the pendant amine and amide groups of NACHI plays a vital role in the selective dispersion of semiconductor nanotubes and debundling down to individual nanotube size or thin bundles of 2–3 nanotubes. The very low intensity of disorder induced D-band at 1298 cm^{-1} for SWNT–NACHI supernatant shows that the polymer is physically attached on the nanotube surface without altering the intrinsic electronic structure [41].

In Fig. 5d, the distinct fluorescence peaks in the Raman spectrum of SWNT–NACHI suspension at near infrared region represents emissions from (6, 4), (9, 1), (8, 3), (6, 5) and (7, 5) nanotubes, which again demonstrate that the nanotubes are isolated into individual tubes or thin bundles consisting of 2–3 nanotubes, and are well dispersed. The fluorescence band intensity was considerably weak for SWNT–SDBS supernatant suspension, while the SWNT–NACHI suspensions marked relatively high intensity fluorescence bands. It can be attributed to the presence of individual as well as thin bundles of semiconductor-enriched nanotubes in SWNT–NACHI supernatant, because the fluorescence emission from inter-band transitions can only be observed for individually dispersed semiconducting SWNTs [42]. Therefore, our results illustrate that the water soluble NACHI has a capability for effective dispersion of SWNTs as individual tubes and thin bundles in neutral pH medium and possess selective adsorption on semiconducting nanotubes.

The FT-IR spectra of the NACHI and the SWNT–NACHI complex are shown in Fig. 6. The sample for FT-IR analysis was prepared by drop casting thin films of NACHI and SWNT–NACHI suspension on Si substrate at room temperature and dried under atmospheric conditions. The polymer peak shift in the FT-IR spectra provides information about the charge transfer between SWNT and the NACHI. An up-shift in the $-NH_2$ bending mode vibration from 1655 cm^{-1} in NACHI sample to 1659 cm^{-1} in the SWNT–NACHI is due to charge transfer from lone pair of electron on the N-groups of the NACHI to the SWNT because of the partial escape of electrons from the low lying anti-bonding acceptor orbital [43].

Finally, electrical characterization of thin films was conducted by measuring the current–voltage (I_{ds}–V_{gate} and I_{ds}–V_{ds}) characteristics. The channel length and width of the devices were 500 and 300 μm respectively, and Au contact electrodes were deposited by thermal evaporation. The average density of nanotubes in the devices was ~40/μm^2. Fig. 7a displayed a p-type characteristic of SWNT–NACHI device. The on off ratio of the device was estimated to be 4.7×10^2. The comparison of *I–V* curves of SWNT–SDBS supernatant and SWNT–NACHI supernatant thin films prepared on glass substrate illustrated a linear shape for former and a non-linear shape for the latter (Fig. 7b). The non-ohmic behavior of SWNT–NACHI thin film illustrates that it mainly consists of semiconducting nanotubes. In addition, the current was decreased in two orders magnitude for SWNT–NACHI film compared to that in SWNT–SDBS film, further illustrates the semiconductor property of SWNT–NACHI sample.

4. Summary

In this study we demonstrated the effective debundling and selective dispersion of semiconducting SWNTs using a neutral pH water soluble chitosan derivative, N-acetylated chitosan. The chitosan derivative was prepared by controlled N-acetylation of chitosan with acetic anhydride and the functionalization was confirmed by FT-IR spectroscopy. Evaluation of SWNT–NACHI dispersion demonstrated that the supernatant dispersion of individualized SWNTs is enriched with semiconducting nanotubes due to preferential adsorption of N-groups of the NACHI on semiconducting nanotubes. The neutral pH aqueous dispersion of well isolated nanotubes with semiconducting properties acquired by wrapping with a biocompatible polymer opens up new prospects for the SWNT-biomacromolecule hybrids, drug delivery, cell culture and biosensor applications.

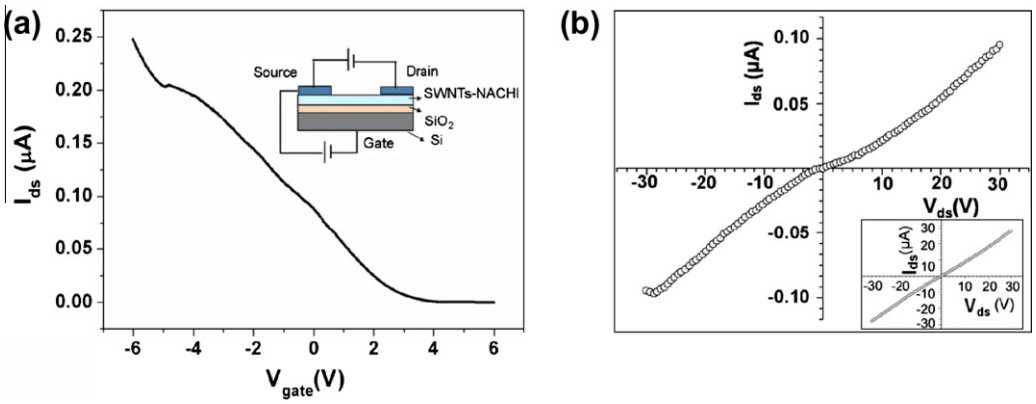

Fig. 7. Current–voltage characteristics of SWNT–NACHI supernatant thin film. (a) I_{ds}–V_{gate} and (b) I_{ds}–V_{ds}. The inset of image (a) shows schematic of a FET device. The inset of image (b) shows a linear *I–V* characteristic of SWNT–SDBS supernatant thin film.

Acknowledgments

This research was supported by a Grant (A090902) from Gyeonggi Technology Development Program funded by Gyeonggi Province. In addition, we thank the BK21 program of molecular science and technology in Ajou University.

References

[1] P.M. Ajayan, Chem. Rev. 99 (1999) 1787.
[2] J. Bernholc, D. Brenner, N.M. Buongiorno, V. Meunier, C. Roland, Annu. Rev. Mater. Res. 32 (2002) 347.
[3] M. Endo, M.S. Strano, P.M. Ajayan, in: A. Jorio, G. Dresselhaus, M.S. Dresselhaus (Eds.), Topics in Applied Physics, Springer, Berlin/Heidelberg, 2008, p. 13.
[4] X. Han, D.C. Janzen, J. Vaillancourt, X. Lu, Micro & Nano Lett. 2 (2007) 96.
[5] Q. Cao, S.H. Hur, Z.T. Zhu, Y. Sun, C. Wang, M.A. Meitl, M.S. Shim, J.A. Rogers, Adv. Mater. 18 (2006) 304.
[6] L. Vaisman, H.D. Wagner, G. Marom, Adv. Colloid Interface Sci. 128–130 (2006) 37.
[7] D. Tasis, N. Tagmatarchis, V. Georgakilas, M. Prato, Chem. Eur. J. 9 (2003) 4000.
[8] K. Balasubramanian, M. Burghard, Small 1 (2005) 180.
[9] S. Ghosh, C.N.R. Rao, Nano Res. 2 (2009) 183.
[10] M.S. Strano, C.A. Dyke, M.L. Usrey, P.W. Barone, M.J. Allen, H. Shan, C. Kitrell, R.H. Hauge, J.M. Tour, R.E. Smalley, Science 301 (2003) 1519.
[11] S. Campidelli, M. Menegheti, M. Prato, Small 3 (2007) 1672.
[12] R.J. Chen, Y. Zhang, D. Wang, H. Dai, J. Am. Chem. Soc. 123 (2001) 3838.
[13] V.C. Moore, M.S. Strano, E.H. Haroz, R.H. Hauge, R.E. Smalley, Nano Lett. 3 (2003) 1379.
[14] H. Wang, Curr. Opin. Colloid Interface Sci. 14 (2009) 364.
[15] D.M. Delozier, K.A. Watson, J.G. Smith Jr., T.C. Clancy, J.W. Connell, Macromolecules 39 (2006) 1731.
[16] K.K. Kim, S.M. Yoon, J.Y. Choi, J. Lee, B.K. Kim, J.M. Kim, J.H. Lee, U. Paik, M.H. Park, C.W. Yang, K.H. An, Y. Chung, Y.H. Lee, Adv. Funct. Mater. 17 (2007) 1775.
[17] L. Vaisman, G. Marom, H.D. Wagner, Adv. Funct. Mater. 16 (2006) 357.
[18] R. Krupke, F. Hennrich, H. von Lohneysen, M.M. Kappes, Science 301 (2003) 344.
[19] M.S. Arnold, A.A. Green, J.F. Hulvat, S.I. Stupp, M.C. Hersam, Nat. Nanotechnol. 1 (2006) 60.
[20] T. Tanaka, H. Jin, Y. Miyata, H. Kataura, Appl. Phys. Exp. 1 (2008) 114001 (3pp).
[21] T. Tanaka, H. Jin, Y. Miyata, S. Fujii, H. Suga, Y. Naitoh, T. Minari, T. Miyadera, K. Tsukagoshi, H. Kataura, Nano Lett. 9 (2009) 1497.
[22] P.G. Collins, M.S. Arnold, P. Avouris, Science 292 (2001) 706.
[23] H. Li, B. Zhou, Y. Lin, L. Gu, W. Wang, K.A. Shiral Fernando, S. Kumar, L.F. Allard, Y.P. Sun, J. Am. Chem. Soc. 126 (2004) 1014.
[24] D. Chattopadhyay, I. Galeska, F. Papadimitrakopoulos, J. Am. Chem. Soc. 125 (2003) 3370.
[25] Q. Cao, H. Kim, N. Pimparkar, J.P. Kulkarni, C. Wang, M. Shim, K. Roy, M.A. Alam, J.A. Rogers, Nature 454 (2008) 495.
[26] A. Ishibashi, N. Nakashima, Bull. Chem. Soc. Jpn. 79 (2006) 357.
[27] Y. Liu, L. Gao, S. Zheng, Y. Wang, Nanotechnology 18 (2007) 365702 (6pp).
[28] D. Nepal, K.E. Geckeler, Small 2 (2006) 406.
[29] S. Ozarkar, M. Jassal, A.K. Agrawal, Fibers Polym. 9 (2008) 410.
[30] D. Douroumis, D.G. Fatouros, N. Bouropoulos, K. Papagelis, D. Tasis, Int. J. Nanomed. 2 (2007) 761.
[31] S. Lu, X. Song, D. Cao, Y. Chen, K. Yao, J. Appl. Polym. Sci. 91 (2004) 3497.
[32] K.V. Harish Prashanth, R.N. Tharanathan, Trends Food Sci. Technol. 18 (2007) 117.
[33] T. Takahashi, C.R. Luculescu, K. Uchida, T. Ishii, H. Yajima, Chem. Lett. 34 (2005) 1516.
[34] H. Yang, S.C. Wang, P. Mercier, D.L. Akins, Chem. Commun. 13 (2006) 1425.
[35] L.Y. Yan, Y.F. Poon, M.B. Chan-Park, Y. Chen, Q. Zhang, J. Phys. Chem. C 112 (2008) 7579.
[36] M.C. LeMieux, M. Roberts, S. Barman, Y.W. Jin, J.M. Kim, Z. Bao, Science 321 (2008) 101.
[37] C. Wang, J. Zhang, K. Ryu, A. Badmaev, L.G. De Arco, C. Zhou, Nano Lett. 9 (2009) 4285.
[38] P. Bonnet, M. Gresil, H. Bizot, I. Riou, P. Bertoncini, A. Buleon, O. Chauvet, J. Nanoparticles Res. 12 (2010) 545.
[39] T. Fujigaya, T. Fukumaru, N. Nakashima, Synth. Met. 159 (2009) 827.
[40] C.A. Furtado, U.J. Kim, H.R. Gutierrez, L. Pan, E.C. Dickey, P.C. Eklund, J. Am. Chem. Soc. 126 (2004) 6095.
[41] S. Manivannan, I.O. Jeong, J.H. Ryu, C.S. Lee, K.S. Kim, J. Jang, K.C. Park, J. Mater. Sci.: Mater. Electron. 20 (2009) 223.
[42] D.H. Shin, J.E. Kim, H.C. Shim, J.W. Song, J.H. Yoon, J.D. Kim, S. Jeong, J. Kang, S.H. Baik, C.S. Han, Nano Lett. 8 (2008) 4380.
[43] K.E. Wise, C. Park, E.J. Siochi, J.S. Harrison, Chem. Phys. Lett. 391 (2004) 207.